Journal of Crystal Growth 540 (2020) 125652

Contents lists available at ScienceDirect

Journal of Crystal Growth

journal homepage: www.elsevier.com/locate/jcrysgro

Controlled growth of InGaN quantum dots on photoelectrochemically etched InGaN quantum dot templates

Syed Ahmed Al Muyeed*[,1], Xiongliang Wei[1], Damir Borovac, Renbo Song, Nelson Tansu*, Jonathan J. Wierer Jr.*

Center for Photonics and Nanoelectronics, Department of Electrical and Computer Engineering, Lehigh University, Bethlehem, PA 18015, USA

ARTICLE INFO

Communicated by R.M. Biefeld

Keywords:
A1. Atomic force microscopy
A1. Photoelectrochemical etching
A3. Metalorganic chemical vapor deposition
A3. Quantum dots
B1. Nitrides
B3. Light emitting diodes

ABSTRACT

Controlled growth of InGaN quantum dots (QDs) using photoelectrochemically (PEC) etched InGaN QD templates is demonstrated. The InGaN QDs are grown by a self-assembly (SA) method using metal-organic chemical vapor deposition on templates consisting of planar GaN and PEC etched InGaN QDs for comparison. The InGaN QD templates are formed using quantum-size-controlled PEC etching of planar InGaN layers on GaN, which produces controlled QD radiuses with a statistical mean (μ) of 17.3 nm and standard deviation (σ) of 6.2 nm, and densities of 1.2×10^{10} cm^{-2}. The PEC etched QDs are capped with an AlGaN interlayer and GaN barrier layer to recover a planar surface morphology for subsequent SA growth of QDs. The PEC QD templates behave as seeds via localize strain near the PEC QDs which provide improved control of the SA QD growth. The SA grown QDs on PEC QD templates are smaller and have controlled radiuses with $\mu = 21.7$ nm and $\sigma = 11.7$ nm compared to the SA QDs on planar GaN templates with radiuses of $\mu = 37.8$ nm and $\sigma = 17.8$ nm. Additionally, the dot densities of the SA QDs on PEC QD templates are ~3 times higher and more closely match the underlying densities of the template (8.1×10^9 cm^{-2}). Multiple quantum dots (MQDs) are also grown on both templates that consist of 4 periods of SA QDs and AlGaN/GaN interlayer/barrier layers. The MQDs grown on PEC QD templates better retain their planarized smooth surfaces after barrier layer growth, and exhibit ~3 times stronger PL intensity at room temperature compared to MQDs grown on planar GaN.

1. Introduction

The advantages of quantum dots (QDs) for light emitters are well known and are a result of the strong modification of the electronic density of states [1–3]. Laser diodes (LDs) using epitaxially formed QDs can have lower carrier (or current) transparency and higher differential gain [4,5]. Indeed, the lowest current threshold lasers use epitaxial QDs as the light active layer [6,7]. QDs not only impact optical gain and stimulated emission, but also the spontaneous emission present in light-emitting diodes (LEDs) [3]. As one would expect from the relationship between optical gain and spontaneous emission, there is also an improvement in spontaneous emission when substituting QDs for quantum wells. Indeed, it has been shown theoretically that there should be an improvement in the efficiency of III-nitrides LEDs using QDs [8,9]. In fact, it is also possible that Auger recombination will be reduced in QD active layers as observed in colloidal QDs of various materials [10,11]. Beyond the traditional light emitters, QDs with their atom-like behavior are also useful for other applications such as creating single-photon sources for quantum computing [1,12].

For both LEDs and LDs, the benefits of QDs are amplified as the size and energy distribution of the QD ensembles becomes more uniform and the dot density is increased [13]. In the synthesis of epitaxial QDs, which is the focus here, there is great difficulty in precisely controlling QD sizes and densities. The most popular method of growing epitaxial QDs is by Stranski-Krastanov (SK) growth where the strain between the underlying layer and the QD layer leads to 3-dimensional (3D) QD formation, and there are some reports of InGaN QDs grown using this method [14–18]. Volmer–Weber (VW) growth of InGaN QDs where the adatom to adatom interactions are stronger than with the surface are also reported [19–21]. Regardless of the method, these self-assembled (SA) QD growth techniques have some drawbacks. Firstly, the dot density for these methods can be relatively low, and secondly, the QD can vary greatly in size. Alternative ways to fabricate QDs with better size control include selective-area epitaxy and site-controlled reactive-ion etching, but the QD size density is limited by the mask dimensions, and these QDs can also be quite large (~20 nm diameter) [22–24].

* Corresponding authors.
E-mail addresses: sya216@lehigh.edu (S.A. Al Muyeed), tansu@lehigh.edu (N. Tansu), jwierer@lehigh.edu (J.J. Wierer).
[1] Equal contributors.

https://doi.org/10.1016/j.jcrysgro.2020.125652
Received 4 December 2019; Received in revised form 29 February 2020; Accepted 3 April 2020
Available online 08 April 2020

Recently a new method has been developed to synthesize more uniform InGaN QDs called quantum-size-controlled photo-electrochemical (PEC) etching [25–27]. In this method, InGaN QDs are formed from planar epitaxial InGaN layers on GaN in an electrochemical cell. The samples are placed in an electrolyte solution under a bias, and coherent laser light is shone on the sample. Only the InGaN layer absorbs the light and the bias attracts the electrolyte to etch the InGaN through oxidation and reduction process [28]. The etch self-terminates when the InGaN layer eventually forms into small enough InGaN QDs that can no longer absorb the exciting light. This method provides great control and tunability of the QD sizes by varying the laser wavelength and In composition of the InGaN layer [27,28]. Although the QDs synthesized in this method are very uniform in size and can have high dot density (10^{11} cm^{-2}), the disadvantage of this approach is that the QDs are exposed to air and this leads to very high non-radiative surface recombination [27]. Therefore, passivation layers are required and have proven to help recover luminescence [29]. Another drawback of this method is it only forms a single QD layer, while multiple layers of QDs (MQDs) are required for lasers and LEDs to provide enough gain and spontaneous emission, respectively.

In this work, epitaxial QDs are formed by SA growth on planar GaN and PEC InGaN QD templates to compare the QD geometries and luminescent properties. The PEC QD templates are formed by first etching the InGaN QDs and then growing thin AlGaN/GaN barrier layers that planarize the surface. Single layers of SA QDs grown on PEC QDs are smaller sized and higher QD density than the SA QDs grown on planar GaN templates, more closely mimicking the original sizes and densities of the PEC QDs. Also, MQDs are formed and compared on both templates, using AlGaN/GaN IL/barrier layers which are optimized to separate, passivate, and planarize the QD layers. MQDs grown on PEC QD templates show better surface morphologies and have ~3 times higher room temperature photoluminescence (PL) intensity compared to SA QD growth on planar GaN.

2. Experimental details

All the samples are grown by metal-organic chemical vapor deposition (MOCVD) on commercial planar n-type GaN on patterned sapphire substrates at 200 Torr. Two different QD structures are investigated and shown schematically in Fig. 1. The first structure (Fig. 1(a)) is self-assembled (SA) InGaN QD layers grown directly on the planar GaN templates. The SA InGaN QDs are grown at 630 °C with a relatively low V/III of ~4200 and a high In/(In + Ga) molar gas phase ratio of 0.50 [30]. The SA QDs are capped with AlGaN interlayers (ILs)

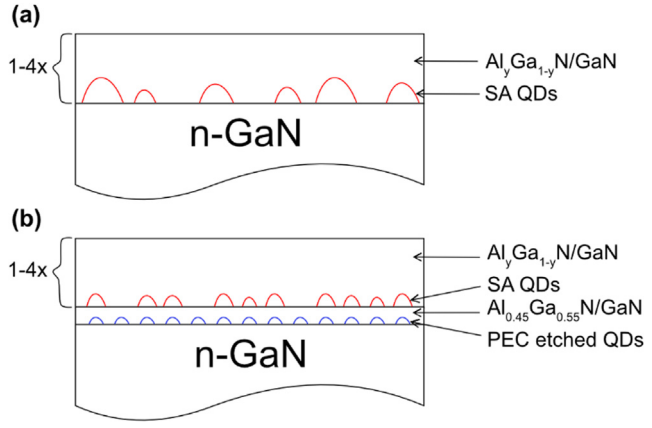

Fig. 1. Schematic cross section of self-assembled (SA) InGaN quantum dots (QDs) grown on (a) planar GaN, and (b) photo-electrical chemically (PEC) etched InGaN QD templates. In some instances, the QDs are capped with $Al_yGa_{1-y}N$ interlayers (IL) and GaN barrier layers. Also, structures are grown with 2 or 4 periods the QD/IL/barrier layers.

also at 630 °C followed by an increase in temperature to 830 °C to grow the GaN barrier layers. The $Al_yGa_{1-y}N$ composition is varied by varying the molar gas phase ratio of Al/(Al + Ga) and the thickness of the GaN barrier is varied (5 vs 8 nm) to find AlGaN/GaN IL/barrier layers that result in a planarized surface and highest photoluminescence intensity. For the AlGaN IL and GaN barriers the V/III ratio is increased to ~50,000 and ~17,000, respectively, by increasing the NH_3 flow to 3000 sccm from 800 sccm. For MQDs, the temperature is decreased to 630 °C after the GaN barrier layer to form the next layer of QDs, and the QD, IL, and barrier growth sequence is repeated up to 4 times.

The second structure consists of SA QDs grown on PEC QD template layers (as shown in Fig. 1(b)). To form the PEC QDs, a 10 nm thick InGaN layer emitting at 470 nm is grown first. These InGaN layers are subjected to quantum-sized-controlled photo-electrochemical etching [27,29]. This process consists of placing the sample into an electrochemical cell with a 0.2 M H_2SO_4 solution, biased at 1.5 V, and exposed to a 445 nm pulsed laser with an average power density of 100 mW/cm^2 [29]. The PEC QDs are then returned to the MOCVD reactor and capped with 2 nm thick $Al_{0.45}Ga_{0.55}N$ IL and 5 nm thick GaN barrier grown at 730 °C and 905 °C, respectively, to planarize the surface. Then, SA InGaN QDs with AlGaN IL and GaN barriers are grown using the same conditions as on planar GaN to create single and MQD layers.

After growth the surfaces of the samples are characterized by atomic force microscopy (AFM) to determine QD sizes and surface morphology of IL/barrier layers. Photoluminescence (PL) with 405 nm laser diode at 8 K and room temperature, and absorption measurements are performed to compare the luminescent efficiency of the different QD samples. The low temperature PL is used when the QDs are exposed or have less effective IL/barrier layers to overcome large surface recombination losses, while room temperature conditions are used for effectively passivated QDs. X-ray diffraction (XRD) omega-2theta measurements along (0002) reflection of GaN are performed on MQD structures. Due to large beam size the XRD signal samples and averages over areas with and without QDs. Fitting this data with 1-dimensional simulation is performed, and while not precise, it does allow for estimations on In compositions in the $In_xGa_{1-x}N$ QDs. Regardless of the template, $x = 0.25$ is found by fitting the XRD data.

3. Results and discussion

This section is organized as follows. First, the SA QD growth on both template layers is explored to find QD layers that are of high QD density and exhibit the best photoluminescence. Then, an effective set of AlGaN IL and GaN barrier layers are investigated to retain the high luminescence and also planarize the QD layer for subsequent QD growth. Finally, SA MQDs are grown on both template layers and the QD sizes, densities, and luminescence of these layers are compared.

3.1. Self-assembled quantum dots on planar GaN

The SA QD growth time is varied to determine the sizes, densities, and luminescent properties of the QDs. Fig. 2 shows the AFM images of uncapped SA QDs grown for (a) 30, (b) 45, and, (c) 60 sec on planar GaN. The QD density increases as the growth time increases, and the 60 sec sample has QDs that begin to coalesce with each other. The SA QD growth on planar GaN results in a large variation in the dot dimensions. For example, the 45 sec sample has QD radiuses that vary from 10 to 75 nm and a density of 2.8×10^9 cm^{-2}. Fig. 2(d) shows the PL intensity of the samples at 8 K. The peak PL intensities are 470 nm and 500 nm for the 30 sec and 45 sec samples, respectively, and the longer wavelength light is the GaN "yellow band". The PL intensity is highest for the 45 sec sample and is lower for the other two samples. Based on the high QD density, separation in QDs, and highest PL intensity a growth time of 45 sec is used for the rest of this study.

Next, $Al_yGa_{1-y}N$ IL and a GaN barrier layers are investigated to passivate the SA QDs, and planarize the surface for subsequent QD

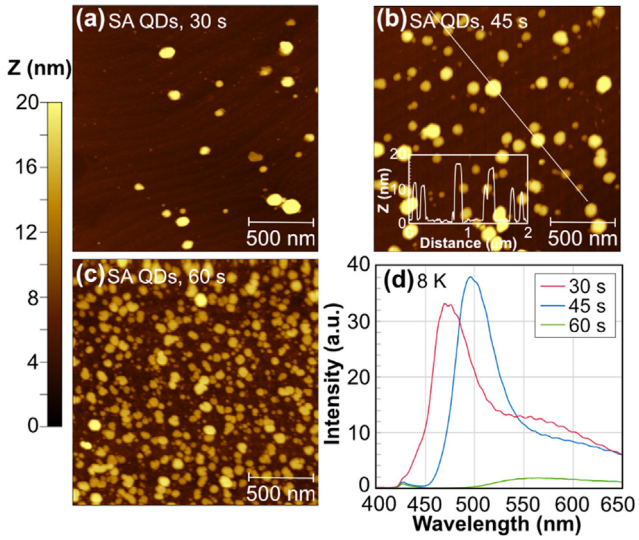

Fig. 2. Atomic force microscope (AFM) images of self-assembled (SA) InGaN quantum dots grown on planar GaN for (a) 30 sec, (b) 45 sec, and, (c) 60 sec. SA QDs grow randomly and show large size variation (shown in inset of (b)). Dot density increases with growth time. (d) Photoluminescence (PL) of these samples under the same power density at 8 K reveal that the PL intensity is highest for the growth time of 45 sec.

growth. The choice of using a low temperature $Al_yGa_{1-y}N$ IL as the first layer is based on successful passivation of PEC QDs [29], and also effectiveness at retaining In in high-In content quantum wells [31–34]. Fig. 3 shows the AFM images of the surfaces with different IL/barrier layers grown on top of the SA QDs grown on planar GaN templates. In Fig. 3(a)–(e) the $Al_yGa_{1-y}N$ IL and GaN barrier have target thicknesses (based on growth on planar surfaces) of 2 nm and 5 nm, respectively, and the Al content, *y*, is varied from 0.8 to 0.0. For y = 0.80 the surface is extremely rough with large In inclusions and large intersecting pits emanating from threading dislocations [35]. These In inclusions are verified by removal with HCl etching. Al adatoms have low mobility during growth at low temperatures, and thus at a high Al content the AlGaN IL cannot effectively cover the whole surface of the QDs [36,37]. Therefore, at the raised temperatures for the GaN barrier, the QDs disassociate and In forms on the surface. As Al composition, *y*, is lowered, the In inclusions become gradually less frequent and the surface becomes smoother. Additionally, pits caused by threading dislocations are smaller and more isolated. Of this subset, the $Al_{0.10}Ga_{0.90}N$/GaN IL/barrier exhibits the best planar morphology. With a GaN IL (Fig. 3(f)) the surface worsens with the reoccurrence of In inclusions and larger pitting. This sample has the highest PL intensity possibly due to better light extraction from the rough surface and slightly lower non-radiative recombination (defects) when compared to AlGaN IL at these low growth temperatures. However, the surface morphology of the GaN IL samples makes it non-ideal for subsequent QD layer growth.

As the $Al_{0.10}Ga_{0.90}N$/GaN capping layers showed the best surface morphology, another sample is grown with a 2 nm thick $Al_{0.10}Ga_{0.90}N$ IL and an 8 nm thick GaN barrier (thicker) to observe if the morphology improves. The AFM image of this sample (Fig. 3(g)) shows a very smooth surface with very few In inclusions. Also, the pits are isolated and connected with terraced steps. The morphology of this particular sample is similar to InGaN/GaN multiple quantum wells showing that the non-planar SA QD surface can be recovered [34,38].

Finally, Fig. 3(h) shows the PL intensity of this set of samples measured at 8 K with an input laser power density (~830 W/cm^2). The samples with y = 0.1 and y = 0 exhibit the highest PL intensity. Given the high PL intensity and best morphology, the 2 nm/8 nm thick $Al_{0.10}Ga_{0.90}N$/GaN IL/barrier is chosen for the growth of multiple quantum dot (MQD) active regions in this study.

The chosen growth conditions for the SA QDs and IL/barrier layers are then used to form MQD structures. Fig. 4(a) shows an AFM image of 2 layers of SA QDs (2x) where the first QD layer is capped with $Al_{0.10}Ga_{0.90}N$/GaN IL/barrier, and the second top QD layer does not have an IL/barrier (bare). The second QD layer still results in QDs, but they are not as well formed as the first layer (compare to Fig. 2(b)) as they form in clusters and merge with each other. Fig. 4(b) shows the AFM image of 4 layers of SA QDs (4x) with $Al_{0.10}Ga_{0.90}N$/GaN IL/barriers. The topmost surface is capped with an IL/barrier for comparison to the capped single SA QD layer, shown in Fig. 2(g). For the MQD, the surface morphology has degraded significantly with the

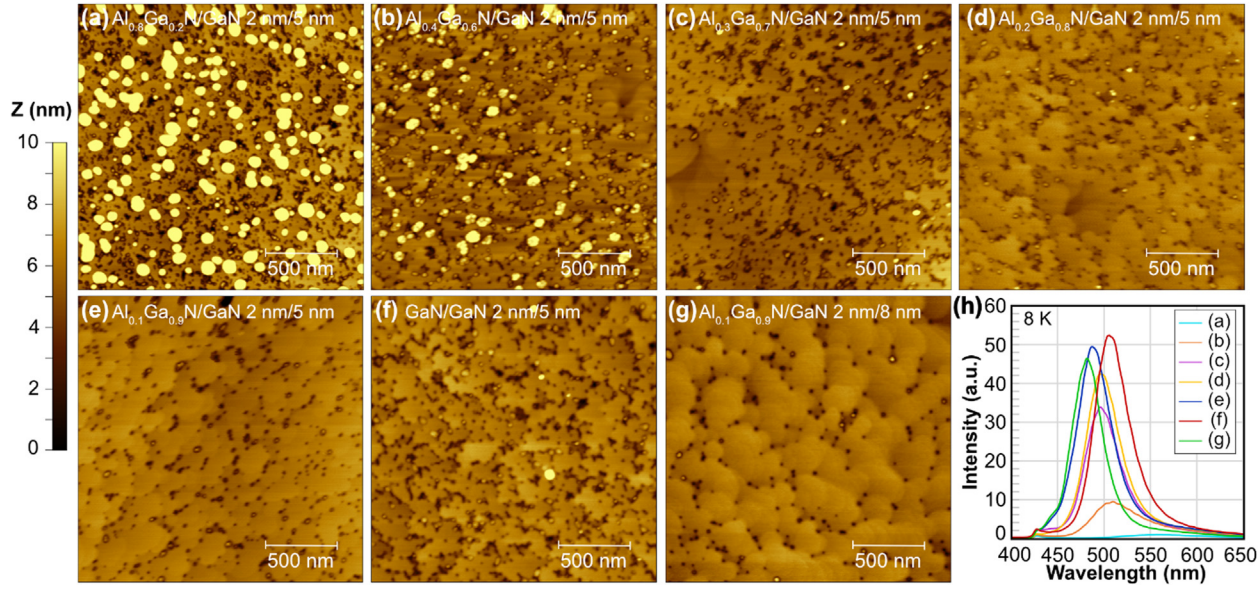

Fig. 3. AFM images of SA quantum dots (QDs) capped with 2 nm/5 nm $Al_yGa_{1-y}N$/GaN IL/barrier layers with different Al compositions, *y*, (a) 0.80, (b) 0.40, (c) 0.30, (d) 0.20, and (e) 0.10. As *y* is gradually decreased the surface becomes smoother and the In inclusions reduce in number. For (f) *y* = 0.0, the SA dots are capped with 2 nm/5 nm thick GaN IL/barrier layers, and the surface again becomes rough with increased in V-pits and In inclusions. For (g), the SA dots are capped with a 2 nm/8 nm thick $Al_{0.10}Ga_{0.90}N$/GaN IL/barrier, and the surface looks the best with no In inclusions and well-formed V-pits. (h) The PL of all samples at 8 K under the same power density.

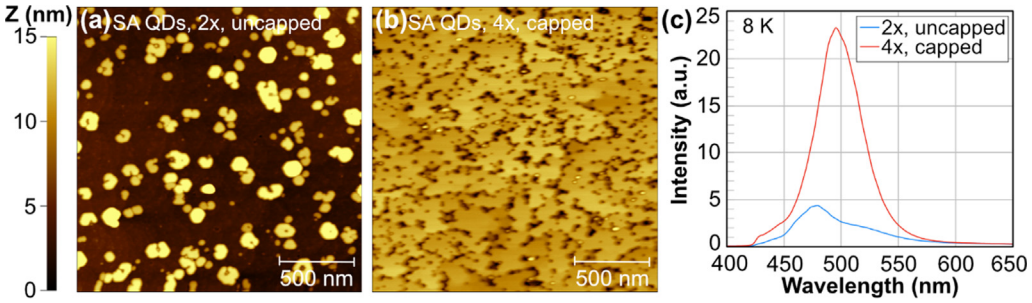

Fig. 4. AFM images of (a) an uncapped surface of 2 layers (2x) of self-assembled (SA) InGaN quantum dots (QDs) and, (b) capped surface of 4 layers (4x) of SA QDs grown on planar GaN. For the 4x multiple QD structure, the surface is rougher than a single QD layer and has In inclusions. (c) PL of the two samples at 8 K. The 4x capped InGaN QDs show ~6 times higher PL intensity than the uncapped 2x sample.

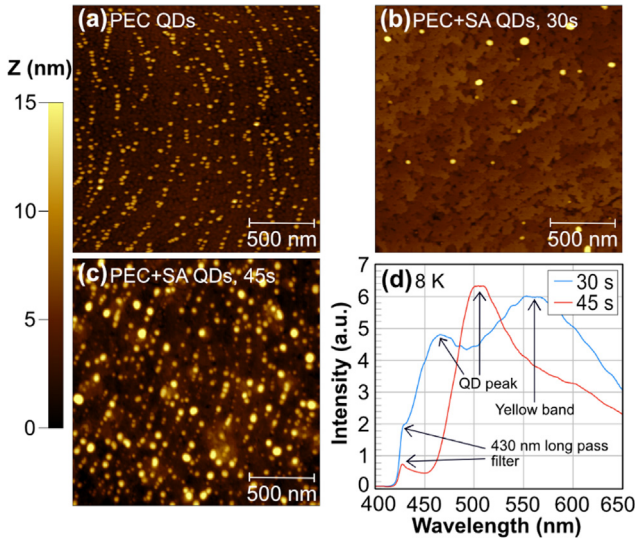

Fig. 5. AFM images of (a) PEC etched InGaN QDs, and single layers of uncapped SA QDs grown for (b) 30 sec and (c) 45 sec on PEC etched QDs. The SA QDs form along the atomic steps (c) the same as the PEC etched QDs, suggesting that the PEC etched QDs act as seeds. (d) PL for SA QDs grown on PEC etched dots at 8 K. For the 45 sec sample the dot density is higher resulting in higher PL intensity.

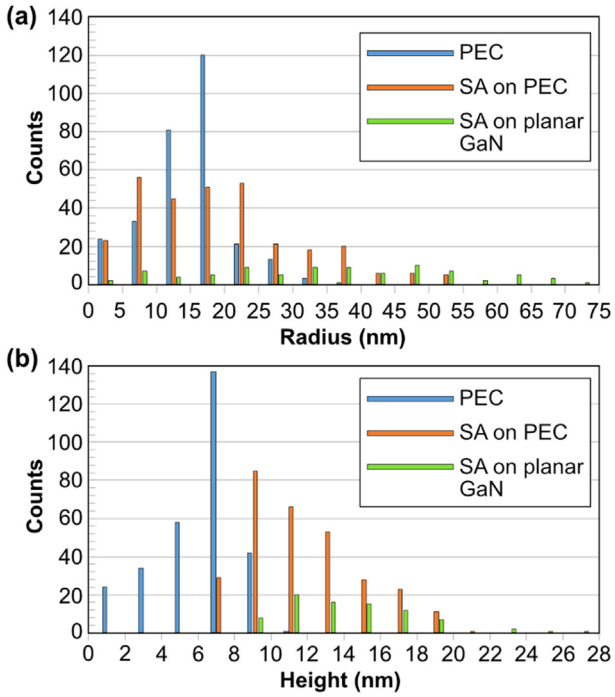

Fig. 6. Distribution of (a) mean radius and (b) maximum height of the QDs. The PEC QDs are very uniform in dot radius and height. Compared to the SA QDs on planar GaN, the SA QDs on PEC QDs are smaller in size and more uniform in size distribution.

presence of larger and intersecting pits. This suggests as QD layers are added to the structure, the thickness of the IL/barrier is not significant enough to recover the planar morphology observed in a single layer. Fig. 4(c) shows the PL intensity of the 2x and 4x MQD samples measured at 8 K and a power density of ~830 W/cm^2. The 4x MQD have much higher PL intensity as expected compared to the 2x MQD. The emission is also redshifted indicating the QDs are becoming larger as subsequent layers are grown.

3.2. Self-assembled InGaN quantum dots on PEC etched InGaN quantum dots

PEC etched InGaN QD templates are developed which consist of PEC InGaN QDs and AlGaN/GaN IL/barrier layers. Fig. 5(a) shows an AFM image of the PEC etched InGaN QD surface. The dot radiuses and heights mainly vary from 15 to 20 nm and 6–10 nm, respectively, and the dot density is 1.2 × 10^{10} cm^{-2}. PEC etched InGaN QDs tend to be much smaller and have much higher QD densities compared to epitaxial InGaN QDs [27]. It is also interesting that the PEC QDs form along the atomic steps forming curved lines of QDs. $Al_{0.45}Ga_{0.55}N$/GaN layers are grown on top of the PEC QDs with target thicknesses (based on growth on planar surfaces) of 2 nm and 5 nm [29]. These layer thicknesses are chosen to effectively cover the QD, but also kept thin enough that the strain of the PEC QDs is still present in the capping layer to influence the growth of subsequently grown SA QDs.

SA QDs are grown on these PEC QD template layers for 30 sec and 45 sec using the same SA growth conditions on planar GaN. The QD density grown for 30 sec, shown in Fig. 5(b), is much lower the QD density for the 45 sec growth shown in Fig. 5(c). There is a remarkable change in the SA QDs growth for 45 sec (Fig. 5(c)) compared to the same growth time on planar GaN (Fig. 2(b)). The QD sizes are much smaller (radiuses and heights mainly vary from 10 to 25 nm and 8–18 nm, respectively) and the QD density is much higher (8.1 × 10^9 cm^{-2}) for the SA QDs grown on PEC QD templates, as compared to the SA QDs on planar GaN (~2.8 × 10^9 cm^{-2}). Furthermore, the total volume of the InGaN QDs grown in the two cases are similar, just their respective arrangements are different.

The closer match to density and size of the SA QDs to the underlying PEC QDs shown that the template is affecting the SA QD growth. This hypothesis is further supported by the similar arrangement of the SA QDs to the PEC QDs which is aligned along arcs just like the PEC QDs (comparing Fig. 5(a) to (c)). This suggests that the SA QDs are vertically aligning to the seed layer of underlying PEC QDs [39]. Therefore, the PEC QD templates are seeding and provide better control for subsequently grown SA QDs. The size distributions of the SA QDs are larger than the PEC QDs and further work is necessary learn how variables such as AlGaN/GaN layer thicknesses, In-content in the QDs, and QD sizes and densities control this vertical alignment.

It should be noted that higher QD densities are possible with SA growth, up to 10^{10} cm^{-2} [17,20,30], and with changes to the growth

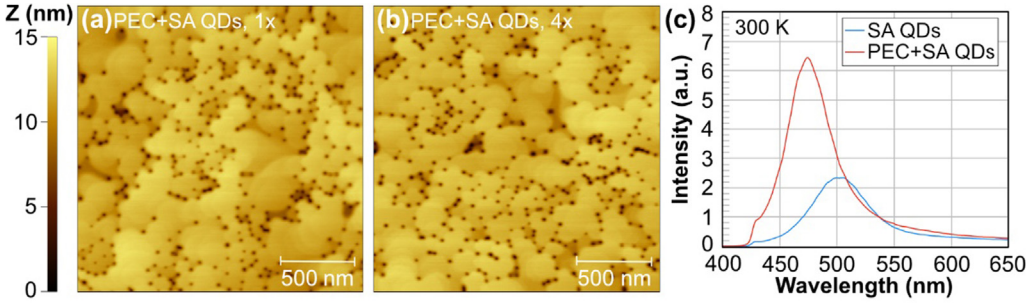

Fig. 7. AFM images of capped (a) single layer (1x) of SA QDs and (b) four layers (4x) of SA multiple quantum dots (MQDs) both grown on PEC QD templates. Unlike the SA QDs grown on planar GaN, the surface morphology for 1x and 4x MQDs look very similar. (c) Room temperature PL of SA MQDs grown on planar GaN and PEC QD templates at the same absorbed power density. The MQD structure grown on PEC QD templates has ~3 times higher intensity and is blue-shifted indicating smaller QD sizes. (For interpretation of the references to colour in this figure legend, the reader is referred to the web version of this article.)

variables similar densities could have been achieved here on planar GaN. However, SA growth on PEC etch QD templates changes the growth approach because the SA QDs are registering to the underlying QDs. The QD densities are now closer to and determined by the underlying QD template, and the sizes by the growth time (total volume of material). It should also be noted that higher densities of PEC etched QDs are possible, so this approach should not present a compromise in QD density.

Fig. 5(d) shows the PL intensity of a single layer of SA QDs grown on PEC QDs for 30 sec and 45 sec at 8 K using the same pump power density. Due to low the QD density of the 30 sec sample most of the pump light is absorbed by the underlying GaN resulting in a stronger yellow-band luminescence. The PL intensity for the 45 sec sample is higher simply due to the higher QD density. The 45 sec growth time is chosen as the optimum for SA QDs on PEC QD templates for MQD structures, similar to SA QDs on planar GaN.

Fig. 6(a) and (b) show the distribution of radius and height for the different QDs determined from the AFMs with single layers of exposed QDs. The PEC QDs in the template are the smallest and most uniform in size providing controlled seed layer for subsequent SA QD growth. The radiuses have a statistical mean (μ) of 17.3 nm and standard deviation (σ) of 6.2 nm, and the heights have μ = 7.1 nm and σ = 2.3 nm. The SA QDs on planar GaN are the largest and show large size variation with μ = 37.8 nm and σ = 17.8 nm for the radiuses and μ = 15.1 nm and σ = 14.1 nm for the heights. On the other hand, the SA QDs on PEC QDs are smaller in size and exhibit a more uniform distribution with μ = 21.7 nm and σ = 11.7 nm for the radiuses and μ12.6 nm and σ = 10.2 nm for the heights. This more controlled SA QD growth is a result of the underlying PEC QDs.

Fig. 7(a) shows an AFM image of a single layer of SA QD layer (1x) grown on PEC QDs. The SA QDs are capped with 2 nm thick $Al_{0.10}Ga_{0.90}N$ IL and 8 nm thick GaN barrier, the same as for the SA QDs on planar GaN. The surface looks very smooth and free of any In inclusions, and the threading dislocation pits are well-formed [34]. Fig. 7(b) shows the AFM image of 4 periods (4x) of SA QDs/$Al_{0.10}Ga_{0.90}N$/GaN grown on a PEC QD template. The surface morphology for the single QD and MQD structures on PEC QDs are similar. Comparing Fig. 7(b) to (b) shows the capping layers are more effective at recovering the SA QDs on PEC QD templates with smoother surfaces, most likely because of the more controlled growth of smaller SA QDs.

Finally, Fig. 7(c) shows the PL intensity of 4 periods of SA MQD grown on planar GaN and PEC QD templates. This measurement is performed at the same absorbed power density since the absorption of the two samples are slightly different at a wavelength (λ) of ~405 nm (~9% for SA QDs on planar GaN and ~7.5% for SA QDs on PEC QDs). This ensures the samples are pumped with the same carrier densities for proper comparison. The PL intensity for the SA MQDs on PEC QDs has ~3 times higher PL intensity compared to the SA MQDs on planar GaN. The SA MQDs on PEC QDs has a peak wavelength of ~470 nm whereas the peak wavelength of the SA MQD on planar GaN is redshifted to ~500 nm. Since the In composition is the same for both QDs the shift is due to the larger SA QDs on planar GaN.

4. Conclusion

In conclusion, SA InGaN QDs are grown on planar GaN and PEC QDs templates. SA InGaN QDs grown on PEC QDs templates show the growth is influenced by the template resulting in smaller size and higher dot density. Additionally, the alignment of the SA QDs are similar to the underlying PEC QDs suggesting the PEC QDs are seeding the SA QD growth. MQDs formed on PEC QD templates shows much smoother and planarized surface morphology because the IL/barrier layers are able to planarize the surfaces and suggests the sizes of the QDs are retained within all the QD layers. All these benefits result in an enhancement of PL compared to SA QDs grown on planar GaN.

CRediT authorship contribution statement

Syed Ahmed Al Muyeed: Investigation, Formal analysis, Writing - original draft. **Xiongliang Wei:** Investigation, Formal analysis. **Damir Borovac:** Investigation. **Renbo Song:** Supervision. **Nelson Tansu:** Supervision. **Jonathan J. Wierer:** Conceptualization, Supervision, Writing - review & editing.

Declaration of Competing Interest

The authors declare that they have no known competing financial interests or personal relationships that could have appeared to influence the work reported in this paper.

Acknowledgements

The authors would like to acknowledge funding from US National Science Foundation (Awards # 1408051, 1505122, and 1708227), and the Daniel E. '39 and Patricia M. Smith Endowed Chair Professorship Fund (N.T.). The work was performed in the Integrated Nanofabrication and Cleanroom Laboratory at Center for Photonics and Nanoelectronics (INCL@CPN).

References

[1] P.M. Petroff, A. Lorke, A. Imamoglu, Epitaxially self-assembled quantom dots, Phys. Today 54 (2001) 46–52, https://doi.org/10.1063/1.1381102.
[2] Y. Arakawa, H. Sakaki, Multidimensional quantum well laser and temperature dependence of its threshold current, Appl. Phys. Lett. 40 (1982) 939, https://doi.org/10.1063/1.92959.
[3] Y.R. Wu, Y.Y. Lin, H.H. Huang, J. Singh, Electronic and optical properties of InGaN quantum dot based light emitters for solid state lighting, J. Appl. Phys. 105 (2009) 013117, https://doi.org/10.1063/1.3065274.
[4] D. Bimberg, M. Grundmann, N.N. Ledentsov, Quantum Dot Heterostructures, John Wiley & Sons, Inc., 1999.
[5] D. Bimberg, N. Kirstaedter, N.N. Ledentsov, Zh.I. Alferov, P.S. Kop'ev, V.M. Ustinov, InGaAs-GaAs quantum-dot lasers, IEEE J. Sel. Top. Quantum Electron. 3 (2) (1997) 196–205, https://doi.org/10.1109/2944.605656.
[6] D. Bimberg, N. Ledentsov, Quantum dots: lasers and amplifiers quantum dots: lasers and amplifiers, J. Phys.: Condens. Matter 15 (2003) R1063–R1076, https://doi.org/10.1088/0953-8984/15/24/201.
[7] G.T. Liu, A. Stintz, H. Li, K.J. Malloy, L.F. Lester, Extremely low room-temperature

threshold current density diode lasers using InAs dots in $In_{0.15}Ga_{0.85}As$ quantum well, Electron. Lett. 35 (14) (1999) 1163–1165, https://doi.org/10.1049/el:19990811.
[8] J.J. Wierer Jr., N. Tansu, A.J. Fischer, J.Y. Tsao, III-nitride quantum dots for ultra-efficient solid-state lighting, Laser Photonics Rev. 10 (4) (2016) 612–622, https://doi.org/10.1002/lpor.201500332.
[9] M. Zhang, P. Bhattacharya, W. Guo, InGaN/GaN self-organized quantum dot green light emitting diodes with reduced efficiency droop, Appl. Phys. Lett. 97 (1) (2010) 11103, https://doi.org/10.1063/1.3460921.
[10] J.L. Pan, Reduction of the Auger rate in semiconductor quantum dots, Phys. Rev. B. 46 (7) (1992) 3977, https://doi.org/10.1103/PhysRevB.46.3977.
[11] I. Robel, R. Gresback, U. Kortshagen, R.D. Schaller, V.I. Klimov, Universal size-dependent trend in Auger recombination in direct-gap and indirect-gap semiconductor nanocrystals, Phys. Rev. Lett. 102 (17) (2009) 177404, https://doi.org/10.1103/PhysRevLett.102.177404.
[12] T.D. Ladd, F. Jelezko, R. Laflamme, Y. Nakamura, C. Monroe, J.L. O'Brien, Quantum computers, Nature 464 (2010) 45–53, https://doi.org/10.1038/nature08812.
[13] M. Winkelnkemper, A. Schliwa, D. Bimberg, Interrelation of structural and electronic properties in $In_xGa_{1-x}N$/GaN quantum dots using an eight-band k·p model, Phys. Rev. B. 74 (2006) 155322, https://doi.org/10.1103/PhysRevB.74.155322.
[14] F. Widmann, B. Daudin, G. Feuillet, Y. Samson, J.L. Rouvière, N. Pelekanos, Growth kinetics and optical properties of self-organized GaN quantum dots, J. Appl. Phys. 83 (1998) 7618, https://doi.org/10.1063/1.367878.
[15] K. Tachibana, T. Someya, S. Ishida, Y. Arakawa, Formation of uniform 10-nm-scale InGaN quantum dots by selective MOCVD growth and their micro-photoluminescence intensity images, J. Cryst. Growth 221 (2000) 576–580, https://doi.org/10.1016/S0022-0248(00)00781-8.
[16] Y.K. Ee, H. Zhao, R.A. Arif, M. Jamil, N. Tansu, Self-assembled InGaN quantum dots on GaN emitting at 520 nm grown by metalorganic vapor-phase epitaxy, J. Cryst. Growth 310 (2008) 2320–2325, https://doi.org/10.1016/j.jcrysgro.2007.12.022.
[17] C. Bayram, M. Razeghi, Stranski-Krastanov growth of InGaN quantum dots emitting in green spectra, Appl. Phys. A 96 (2009) 403–408, https://doi.org/10.1007/s00339-009-5186-2.
[18] B. Damilano, N. Grandjean, S. Dalmasso, J. Massies, Room-temperature blue-green emission from InGan/GaN quantum dots made by strain-induced islanding growth, Appl. Phys. Lett. 75 (1999) 3751, https://doi.org/10.1063/1.125444.
[19] R.A. Oliver, M.J. Kappers, C.J. Humphreys, G.A.D. Briggs, Growth modes in heteroepitaxy of InGaN on GaN, J. Appl. Phys. 97 (2005) 013707, https://doi.org/10.1063/1.1823581.
[20] Q. Wang, T. Wang, J. Bai, A.G. Cullis, P.J. Parbrook, F. Ranalli, Growth and optical investigation of self-assembled InGaN quantum dots on a GaN surface using a high temperature AlN buffer, J. Appl. Phys. 103 (12) (2008) 123522, https://doi.org/10.1063/1.2939568.
[21] C. Meissner, S. Ploch, M. Pristovsek, M. Kneissl, Volmer-Weber growth mode of InN quantum dots on GaN by MOVPE, Phys. Status Solidi. C 6 (52) (2009) S545–S548, https://doi.org/10.1002/pssc.200880872.
[22] G. Liu, H. Zhao, J. Zhang, J.H. Park, L.J. Mawst, N. Tansu, Selective area epitaxy of ultra-high density InGaN quantum dots by diblock copolymer lithography, Nanoscale Res. Lett. 6 (2011) 342, https://doi.org/10.1186/1556-276X-6-342.
[23] L.K. Lee, P.-C. Ku, Fabrication of site-controlled InGaN quantum dots using reactive-ion etching, Phys. Status Solidi C 9 (2012) 609–612, https://doi.org/10.1002/pssc.201100428.
[24] L.K. Lee, L.K. Aagesen, K. Thornton, P.-C. Ku, Origin of broad luminescence from site-controlled InGaN nanodots fabricated by selective-area epitaxy, Phys. Status Solidi A 211 (3) (2014) 531–535, https://doi.org/10.1002/pssa.201330362.
[25] J.M. Hwang, J.T. Hsieh, C.Y. Ko, H.L. Hwang, W.H. Hung, Photoelectrochemical etching of $In_xGa_{1-x}N$, Appl. Phys. Lett. 76 (26) (2000) 3917–3919, https://doi.org/10.1063/1.126820.
[26] X. Xiao, A.J. Fischer, M.E. Coltrin, P. Lu, D.D. Koleske, G.T. Wang, R. Polsky, J.Y. Tsao, Photoelectrochemical etching of epitaxial InGaN thin films: Self-limited kinetics and nanostructuring, Electrochim. Acta 162 (2015) 163–168, https://doi.org/10.1016/j.electacta.2014.10.085.
[27] X. Xiao, A.J. Fischer, G.T. Wang, P. Lu, D.D. Koleske, M.E. Coltrin, J.B. Wright, S. Liu, I. Brener, G.S. Subramania, J.Y. Tsao, Quantum-size-controlled photoelectrochemical fabrication of epitaxial InGaN quantum dots, Nano Lett. 14 (2014) 5616–5620, https://doi.org/10.1021/nl502151k.
[28] X. Xiao, P. Lu, A.J. Fischer, M.E. Coltrin, G.T. Wang, D.D. Koleske, J.Y. Tsao, Influence of pH on the quantum-size-controlled photoelectrochemical etching of epitaxial InGaN quantum dots, J. Phys. Chem. C 119 (2015) 28194–28198, https://doi.org/10.1021/acs.jpcc.5b09555.
[29] X. Wei, S.A. Al Muyeed, M.R. Peart, W. Sun, N. Tansu, J.J. Wierer Jr., Room temperature luminescence of passivated InGaN quantum dots formed by quantum-sized-controlled photoelectrochemical etching, Appl. Phys. Lett. 113 (2018) 121106, https://doi.org/10.1063/1.5046857.
[30] A. Kadir, C. Meissner, T. Schwaner, M. Pristovsek, M. Kneissl, Growth mechanism of InGaN quantum dots during metalorganic vapor phase epitaxy, J. Cryst. Growth 334 (1) (2011) 40–45, https://doi.org/10.1016/j.jcrysgro.2011.08.003.
[31] S.A. Al Muyeed, W. Sun, X. Wei, R. Song, D.D. Koleske, N. Tansu, J.J. Wierer Jr., Strain compensation in InGaN-based multiple quantum wells using AlGaN interlayers, AIP Adv. 7 (10) (2017) 105312, https://doi.org/10.1063/1.5000519.
[32] D.D. Koleske, A.J. Fischer, B.N. Bryant, P.G. Kotula, J.J. Wierer, On the increased efficiency in InGaN-based multiple quantum wells emitting at 530–590 nm with AlGaN interlayers, J. Cryst. Growth 415 (2015) 57–64, https://doi.org/10.1016/j.jcrysgro.2014.12.034.
[33] R. Hashimoto, J. Hwang, S. Saito, S. Nunoue, High-efficiency yellow light-emitting diodes grown on sapphire (0001) substrates, Phys. Status Solidi C 11 (2014) 628–631, https://doi.org/10.1002/pssc.201300433.
[34] S.A. Al Muyeed, W. Sun, M. Peart, R.M. Lentz, X. Wei, D. Borovac, R. Song, N. Tansu, J.J. Wierer Jr., Recombination rates in green-yellow InGaN-based multiple quantum wells with AlGaN interlayers, J. Appl. Phys. 126 (21) (2019) 213106, https://doi.org/10.1063/1.5126965.
[35] F.A. Ponce, S. Srinivasan, A. Bell, L. Geng, R. Liu, M. Stevens, J. Cai, H. Omiya, H. Marui, S. Tanaka, Microstructure and electronic properties of InGaN alloys, Phys. Status Solidi B 240 (2) (2003) 273–284, https://doi.org/10.1002/pssb.200303527.
[36] R. Loganathan, M. Jayasakthi, K. Prabakaran, R. Ramesh, P. Arivazhagan, K. Baskar, Studies on dislocation and surface morphology of $Al_xGa_{1-x}N$/GaN heterostructures grown by MOCVD, J. Alloys Compd. 616 (2014) 363–371, https://doi.org/10.1016/j.jallcom.2014.07.170.
[37] D.G. Zhao, Z.S. Liu, J.J. Zhu, S.M. Zhang, D.S. Jiang, H. Yang, J.W. Liang, X.Y. Li, H.M. Gong, Effect of Al incorporation on the AlGaN growth by metalorganic chemical vapor deposition, Appl. Surf. Sci. 253 (5) (2006) 2452–2455, https://doi.org/10.1016/j.apsusc.2006.04.062.
[38] R. Hashimoto, J. Hwang, S. Saito, S. Nunoue, High-efficiency green-yellow light-emitting diodes grown on sapphire (0001) substrates, Phys. Status Solidi C 10 (11) (2013) 1529–1532, https://doi.org/10.1002/pssc.201300238.
[39] W.S. Liu, H.M. Wu, F.H. Tsao, T.L. Hsu, J.I. Chyi, Improving the characteristics of intermediate-band solar cell devices using a vertically aligned InAs/GaAsSb quantum dot structure, Sol. Energy Mater. Sol. Cells 105 (2012) 237–241, https://doi.org/10.1016/j.solmat.2012.06.023.